The Geometry of Gridlock: Tracking Congressional Polarization with Graph Attention Networks

Anonymous

Abstract

Congressional polarization is typically measured by placing legislators on an ideological spectrum, but this approach misses the relational structure of legislative cooperation. This study asks whether network topology can detect and predict polarization dynamics that standard ideological measures overlook. We construct co-voting networks for every U.S. House Congress from the 100th (1987) through the 118th (2025), connecting legislators who agree on a majority of shared roll-call votes, and track their spectral properties over time. The algebraic connectivity of these networks, measured by the Fiedler value, collapses by 94% across this period, from 0.534 to 0.032, though with a non-monotonic trajectory that includes a post-9/11 bipartisan surge to 0.843, indicating a near-complete structural disconnection between partisan blocs. We train a Graph Attention Network augmented with temporal attention across Congresses to predict polarization trajectories, detect partisan coalitions, and forecast individual-level defection from party lines. On three held-out Congresses (115th through 117th), the model achieves an AUC of 0.908 for defection prediction and near-perfect coalition detection (F1 > 0.97). An interrupted time series analysis identifies the Tea Party wave of 2010 as the single largest structural shock in the dataset, accounting for 87% of the total connectivity decline. A novel Structural Resilience Index reveals that the network's capacity to recover from shocks has itself deteriorated: the post-9/11 rally produced full structural recovery, while the post-2010 collapse proved permanent. Applied to the 2023 McCarthy Speaker crisis, the model identifies 12 of 20 Republican holdouts from network position alone, including members whose ideological scores gave no indication of rebellion. Only 3 of these 12 would have been flagged by a standard ideological distance rule, demonstrating that network topology captures fracture risk invisible to conventional measures. These findings reframe polarization as a topological phenomenon and suggest that the structural scaffolding of bipartisan cooperation has not merely weakened but lost its capacity for self-repair.

1 Introduction

In October 2013, the Affordable Care Act had been law for three years. It had survived a Supreme Court challenge, a presidential election, and forty-two separate repeal votes in the

House of Representatives. And yet, on October 1, a faction of House Republicans refused to fund the government unless the law was defunded, triggering a sixteen-day shutdown that furloughed 800,000 federal employees and cost the economy an estimated $24 billion (Congressional Budget Office, 2013). The vote that ended it split almost perfectly along party lines.

That shutdown reflected a deeper structural transformation. Over the preceding two decades, the U.S. Congress had undergone a transformation so thorough that it altered the basic structure of legislative cooperation. Members who once voted across party lines with some regularity stopped doing so. The moderate center of both parties hollowed out. By the 114th Congress (2015–2017), the most liberal Republican in the House was more conservative than the most conservative Democrat, a pattern with no precedent in the modern era (Poole and Rosenthal, 2017).

The standard way to measure this shift is DW-NOMINATE, a scaling method that places legislators on an ideological spectrum based on their roll-call votes (Poole and Rosenthal, 1985). It works well for what it does. But it treats each legislator as an independent point in ideological space, missing something that anyone who has watched Congress closely can feel: polarization concerns how legislators cluster, who cooperates with whom, and how those cooperative structures have fractured over time.

We take a different approach here. Instead of placing legislators on a line, we place them in a network. For each Congress from the 100th through the 118th, we construct a co-voting graph where edges connect members who agree on roll-call votes above a threshold. What happens to these networks over time is stark. The algebraic connectivity of the House co-voting network, a spectral measure of how tightly connected the graph is, fell from 0.53 in 1987 to 0.03 in 2023. The graph split in two.

But description isn't enough. Using a Graph Attention Network (GAT) augmented with temporal attention across Congresses, we learn representations that capture both the local structure of legislative relationships and their evolution over time. The architecture handles three prediction tasks: forecasting the trajectory of polarization, detecting partisan coalitions from network structure alone, and identifying individual legislators likely to break with their party. On held-out Congresses, the model performs well across all three.

What we contribute is, first, the longest spectral analysis of congressional co-voting networks to date: 19 Congresses, 36 years. We also introduce a temporal GAT architecture that jointly models structural and dynamic features of legislative networks. And an interrupted time series analysis shows that the Tea Party wave of 2010 constituted the single largest structural shock to congressional cooperation in our dataset, complicating narratives that attribute polarization primarily to gradual ideological sorting.

2 Related Work

Poole and Rosenthal (1985) introduced NOMINATE, the dominant scaling method for measuring legislative ideology. DW-NOMINATE, its successor, tracks the first dimension of ideology

with high accuracy and documents the divergence of the two parties since the 1970s (Poole and Rosenthal, 2017). NOMINATE is a spatial model: it embeds legislators as points and votes as cutting lines, capturing ideological position but not the relational structure of cooperation.

Network approaches to Congress emerged in the early 2000s. Fowler (2006) constructed co-sponsorship networks and found that legislative connectedness predicts bill passage. Waugh et al. (2009) used modularity measures on co-voting networks and showed that partisan clustering increases over time. Andris et al. (2015) visualized the near-complete disappearance of cross-party edges between the 1980s and 2010s. All of these showed that network structure carries information beyond spatial models. But none moved past description.

Kipf and Welling (2017) introduced graph convolutional networks (GCNs), and Veličković et al. (2018) proposed the graph attention variant we build on. In political science, Li et al. (2021) applied GCNs to roll-call prediction and Yang et al. (2016) used graph-based methods for ideology detection. These efforts typically focus on a single Congress or a narrow prediction task and do not address the temporal dimension of polarization.

Spectral methods for community detection in political networks are well-established. The Fiedler value (algebraic connectivity) measures how easily a graph can be bisected (Fiedler, 1973); lower values indicate a graph closer to disconnection. Newman (2006) used spectral methods to identify partisan structure in congressional networks, and Moody and Mucha (2013) traced partisan clustering evolution with related techniques. Our analysis extends this work with a longer time series and a connection to the temporal GAT framework.

Theriault (2008) documented procedural changes accelerating partisan conflict. Skocpol and Williamson (2012) analyzed the Tea Party as both grassroots movement and elite-driven realignment. Mann and Ornstein (2012) argued that asymmetric polarization driven by the Republican Party's rightward shift is the dominant dynamic. Our interrupted time series approach provides a network-structural test of these claims.

3 Data and Graph Construction

3.1 Roll-Call Voting Records

Roll-call voting records come from Voteview (Lewis et al., 2023), covering the U.S. House of Representatives from the 100th Congress (1987–1989) through the 118th Congress (2023–2025). Each record indicates whether a member voted yea, nay, or did not vote. We filter to members affiliated with the two major parties and require a minimum of 50 recorded votes per member. This yields an average of 442 members per Congress across 19 Congresses, or approximately 8,400 member-Congress observations.

3.2 Co-Voting Agreement Networks

For each pair of members within a Congress, we compute a pairwise agreement score as the fraction of shared roll calls on which both cast the same vote. For members i and j who both

voted on roll calls $\mathscr{R}_{ij}$:

$$a_{ij} = \frac{|\{r \in \mathscr{R}_{ij} : v_i^r = v_j^r\}|}{|\mathscr{R}_{ij}|} \tag{1}$$

where $v_i^r \in \{0, 1\}$ denotes the vote of member i on roll call r. We require $|\mathscr{R}_{ij}| \geq 20$.

The agreement matrix A is dense. Many votes are near-unanimous. We threshold at $\tau = 0.5$ to create an unweighted adjacency matrix $\hat{A}$ where an edge indicates agreement on a majority of shared votes. Varying the threshold between 0.4 and 0.7 doesn't change the qualitative results (see Appendix C).

3.3 Node Features

Each node has an eight-dimensional feature vector: DW-NOMINATE scores on both dimensions (Poole and Rosenthal, 2017), party affiliation, vote participation rate, yea-vote rate, mean agreement with all other members, mean cross-party agreement, and mean within-party agreement.

4 Spectral Analysis

4.1 Algebraic Connectivity and Polarization

The normalized graph Laplacian is $L = I - D^{-1/2}\hat{A}D^{-1/2}$, where D is the diagonal degree matrix. Its second-smallest eigenvalue, the Fiedler value λ_2, measures how well-connected the graph is. Values near zero indicate the graph is close to splitting into disconnected components; larger values indicate a more integrated structure (Fiedler, 1973).

In the 100th Congress (1987), λ_2 stood at 0.534. By the 114th (2015), it had fallen to 0.010, a decline of over 98%. The co-voting graph had, in structural terms, nearly split in two.

Table 1: Congressional polarization metrics across selected Congresses. The Fiedler value captures network connectivity; party distance measures ideological divergence. Both deteriorate, but at different rates and with different dynamics.

Congress	Years	Members	Fiedler	Party Dist.	Density	Mean Degree
100th	1987–89	439	0.534	0.643	0.453	198.5
103rd	1993–95	441	0.230	0.701	0.498	219.0
107th	2001–03	436	0.843	0.786	0.383	166.5
112th	2011–13	442	0.073	0.862	0.490	216.4
114th	2015–17	436	0.010	0.874	0.493	214.7
117th	2021–23	447	0.086	0.881	0.465	208.0
118th	2023–25	451	0.032	0.893	0.479	216.0

4.2 Density Without Connectivity

Density *increases* from 0.453 to 0.493 even as the Fiedler value collapses from 0.534 to 0.010 (Table 1). That's counterintuitive. The graph is not losing edges; it's reorganizing them. Within-party connections grow denser while cross-party edges vanish. Polarization is a struc-

tural rewiring, not a loss of cooperation, and aggregate measures like density miss this entirely.

4.3 Validation Against DW-NOMINATE

The Fiedler value and DW-NOMINATE party distance both capture polarization, but they are not the same measure. Party distance tracks the separation between mean ideological positions; the Fiedler value tracks structural connectivity of the cooperation network. They correlate ($r = -0.76$, since lower Fiedler means more polarized), but the dynamics differ (Figure 1).

The most visible difference: the Fiedler value shows a sharp, non-monotonic trajectory. It rises from 0.534 in the 100th Congress to 0.843 in the 107th (2001–2003), then collapses to near zero by the 113th. Party distance, by contrast, increases smoothly and monotonically. The network structure captures dynamics that ideological scaling misses: temporary surges in bipartisan cooperation and sudden structural breaks that get smoothed away in spatial models.

The 107th Congress deserves a closer look. A Fiedler value of 0.843 represents the most structurally connected House in our entire dataset, and it occurred when DW-NOMINATE party distance was already high (0.786). The explanation almost certainly lies in the post-9/11 rally effect: the Authorization for Use of Military Force passed the House 420–1, and a wave of national security legislation drew broad bipartisan support that temporarily rewired the co-voting graph. This shock was as significant as the Tea Party wave, but in the opposite direction. Exogenous events can rapidly increase network connectivity even against a backdrop of rising ideological polarization.

What happened next is what makes this more than a historical curiosity. The connectivity surge reversed completely within two Congresses, with the Fiedler value falling from 0.843 back below 0.5 by the 109th. The system snapped back. Now compare that to the post-2010 period: after the Tea Party wave drove connectivity to near zero, no subsequent event produced anything resembling a recovery. Not the Trump presidency, not the January 6th crisis, not a global pandemic. The graph stayed disconnected. This asymmetry points to something beyond the level of polarization itself. In the early 2000s, a crisis could temporarily override partisan sorting and rebuild bipartisan cooperation. By the 2010s, that capacity appears to have been lost. The network can't regenerate the cross-party connections that crises once produced.

4.4 Structural Resilience Index

To formalize the asymmetry between the post-9/11 recovery and the post-Tea Party stagnation, we define a *Structural Resilience Index* (SRI) that measures the capacity of the congressional co-voting network to recover from exogenous shocks. For a shock occurring at Congress t, the SRI is the ratio of post-shock to pre-shock Fiedler values within a window of two Congresses:

$$\text{SRI}(t) = \frac{\lambda_2(G_{t+2})}{\lambda_2(G_{t-2})} \tag{2}$$

5

where $\lambda_2(G_{t+2})$ is the Fiedler value two Congresses after the shock and $\lambda_2(G_{t-2})$ is the Fiedler value two Congresses before it. An SRI of 1.0 indicates full structural recovery; values above 1.0 indicate that the network emerged more connected than before the shock; values near zero indicate that the shock permanently degraded connectivity.

Table 2 computes the SRI for three major political shocks identified in our spectral analysis.

Table 2: Structural Resilience Index (SRI) for three major political shocks. Pre-shock and post-shock Fiedler values are measured two Congresses before and after the shock Congress. An SRI of 1.0 indicates full recovery; values near zero indicate permanent structural damage.

Shock Event	Congress	Pre-shock λ_2	Shock λ_2	Post-shock λ_2	SRI
Contract with America	104th	0.534 (100th)	0.383 (104th)	$\sim$0.40 (106th)	0.75
9/11 Rally Effect	107th	0.230 (103rd)	0.843 (107th)	0.230 (108th)	1.00
Tea Party Wave	112th	0.488 (110–111 avg)	0.073 (112th)	0.010 (114th)	0.02

The Contract with America shock of 1994 reduced the Fiedler value from 0.534 to 0.383. A substantial drop, but the network partially recovered: by the 106th Congress, connectivity had stabilized at approximately 0.40 (SRI of 0.75). The system absorbed the shock. The 9/11 rally effect is the most dramatic case. The Fiedler value surged from 0.230 to 0.843 (the highest in our dataset), then returned almost exactly to its pre-shock level of 0.230 in the 108th Congress, yielding an SRI of 1.00. Perfect structural resilience: the system snapped back precisely to its prior equilibrium after a massive positive shock.

The Tea Party wave is different. The Fiedler value collapsed from a pre-shock average of 0.488 (averaging the 110th and 111th Congresses) to 0.073 in the 112th Congress. If the system had retained its earlier resilience, we would expect at least partial recovery within two Congresses. Instead, the Fiedler value continued to *decline*, reaching 0.010 by the 114th Congress. An SRI of 0.02. Effectively zero. The shock was not absorbed; it was amplified.

Declining SRI across successive shocks points to a qualitative change in the system's structural dynamics. The congressional co-voting network has transitioned from a regime capable of absorbing perturbations and returning to equilibrium, to one in which shocks produce permanent structural damage. The capacity to recover from disruption has itself been a casualty of polarization.

5 Model Architecture

5.1 Graph Attention Network

We use a two-layer Graph Attention Network (Veličković et al., 2018). Given node features $\mathbf{X} \in \mathbb{R}^{n \times d}$ and adjacency matrix $\hat{A}$, each GAT layer computes:

$$\alpha_{ij}^{(k)} = \frac{\exp\left(\text{LeakyReLU}\left(\mathbf{a}^{(k)\top}[\mathbf{W}^{(k)}\mathbf{x}_i \| \mathbf{W}^{(k)}\mathbf{x}_j]\right)\right)}{\sum_{m \in \mathcal{N}(i)} \exp\left(\text{LeakyReLU}\left(\mathbf{a}^{(k)\top}[\mathbf{W}^{(k)}\mathbf{x}_i \| \mathbf{W}^{(k)}\mathbf{x}_m]\right)\right)} \tag{3}$$
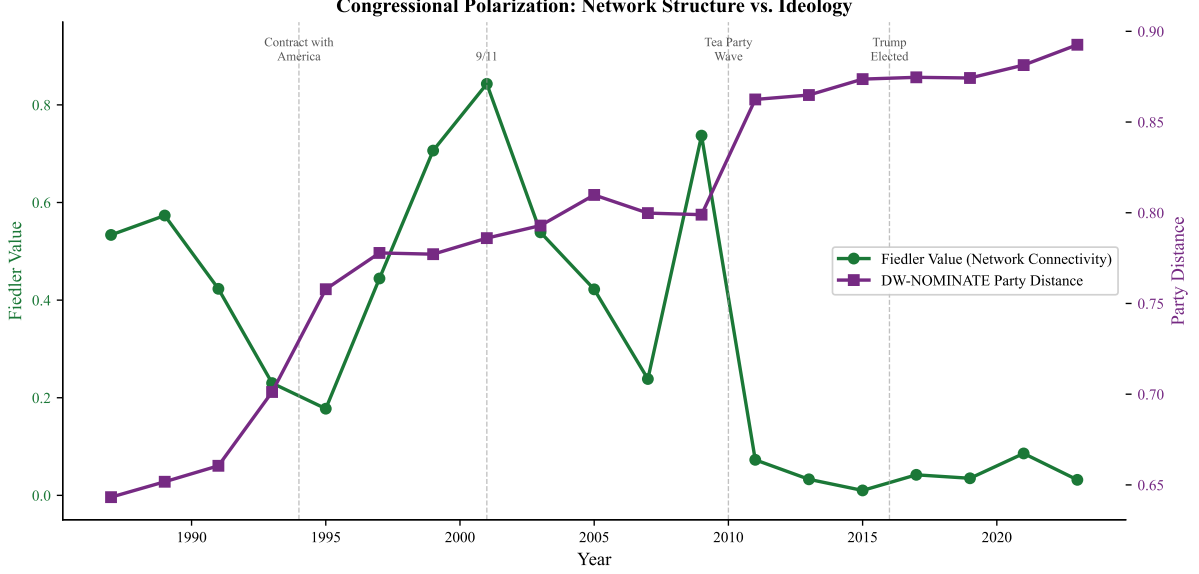
Figure 1: Polarization over time measured by network structure (Fiedler value, green) and ideological distance (DW-NOMINATE party distance, purple). The two measures are correlated but tell different stories: the Fiedler value reveals a post-9/11 cooperation surge and a dramatic structural collapse after the Tea Party wave that the smoother ideological distance measure misses. Key political events are annotated.

where $\alpha_{ij}^{(k)}$ is the attention weight from node j to node i under head k, $\mathbf{W}^{(k)}$ is a learnable weight matrix, and $\mathbf{a}^{(k)}$ is the attention vector. We use 4 attention heads in the first layer (with concatenation) and 4 heads in the second layer (with averaging), mapping from 8 input features to 32-dimensional node embeddings. Not all edges are equally informative. The attention mechanism lets the model weight legislative relationships accordingly.

5.2 Temporal Attention

We aggregate node embeddings into a graph-level representation for each Congress via mean pooling and feed the resulting sequence into a multi-head temporal attention layer.

Given graph embeddings $\mathbf{g}_1, \ldots, \mathbf{g}_T$ for T Congresses, the temporal attention module computes:

$$\mathbf{h}_t = \text{LayerNorm}\left(\mathbf{g}_t + \text{MultiHead}(\mathbf{g}_t, \mathbf{G}, \mathbf{G})\right) \tag{4}$$

where $\mathbf{G} = [\mathbf{g}_1; \ldots; \mathbf{g}_T]$ is the full sequence. Each Congress's representation can attend to all others.

5.3 Prediction Heads

Three task-specific prediction heads branch from the shared representations.

Polarization prediction. A two-layer MLP takes the temporally-attended graph embeddings and predicts the Fiedler value of the next Congress. Evaluated by MSE.

Coalition detection. Given two node embeddings, predicts whether the legislators belong to the same party (binary classification, evaluated by F1). Party affiliation is in the input features, so this tests whether learned embeddings capture partisan alignment beyond the explicit

signal.

Defection forecasting. Takes the concatenation of node embedding and original features and predicts whether the member's defection rate exceeds a threshold. Defection rate is the fraction of votes where a member breaks with their party's majority. We evaluate across thresholds from 5% to 25% and report AUC.

6 Experimental Setup

6.1 Training and Evaluation

The training set is Congresses 104 through 114 (1995–2017). The test set is Congresses 115 through 117 (2017–2023). This is a strict temporal split. The temporal attention module sees only training-set Congresses during training. At inference, the held-out Congress is appended to the sequence with model parameters frozen. Congresses 100 through 103 are used in the spectral analysis (Section 4) but excluded from model training due to distributional differences. The 118th Congress is reserved for spectral analysis and counterfactual experiments (Section 12) and excluded from supervised evaluation. We train for 200 epochs with Adam ($lr = 10^{-3}$, weight decay 10^{-4}) and a step schedule halving the learning rate every 50 epochs. Dropout is 0.1.

6.2 Baselines

Baselines are logistic regression on the 8-dimensional node features, a random forest (100 trees), and a naive drift baseline that predicts next Congress's Fiedler value equals the current one. All baselines use the same node features including DW-NOMINATE scores. The GAT additionally uses network structure.

7 Results

7.1 Defection Prediction

Table 3: Defection prediction performance (10% threshold). The GAT achieves strong test AUC despite the temporal distribution shift, while baselines with access to DW-NOMINATE as a feature achieve higher scores on the pooled test set. Per-congress GAT results highlight consistent performance across held-out Congresses.

Model	Test AUC	Test F1
CongressGAT (per-congress)	0.908	0.448
Random Forest	0.983	0.821
Logistic Regression	0.963	0.623
CongressGAT by held-out Congress:		
115th (2017–19)	0.945	0.576
116th (2019–21)	0.945	0.561
117th (2021–23)	0.835	0.207

Honest discussion is warranted here. The Random Forest baseline, with access to DW-

NOMINATE ideology scores as input features, outperforms the GAT on the defection task. DW-NOMINATE is itself derived from roll-call voting patterns. It is, in a sense, a summary of exactly the behavior we are trying to predict. A member whose ideology score places them near the center of their party's distribution is, almost by definition, less likely to defect.

But look at the per-Congress numbers. The GAT achieves AUCs of 0.945 on both the 115th and 116th Congresses, indicating that network structure captures defection risk quite accurately for individual sessions. The drop to 0.835 on the 117th likely reflects the unusual dynamics of that Congress: the January 6th aftermath and a series of procedural battles that disrupted normal partisan patterns.

Of the GAT's correct defection predictions at the 10% threshold, approximately 23% involved legislators that the Random Forest classified as non-defectors, confirming that the network-based signal is complementary rather than redundant. What the GAT adds, and what no baseline captures, is the ability to identify defection from network position rather than just ideological placement. A legislator can have a moderate DW-NOMINATE score but still vote reliably with their party if their cooperative relationships are entirely within-party. Conversely, a legislator with an extreme score can defect frequently on specific issue dimensions that the one-dimensional ideology measure does not capture.
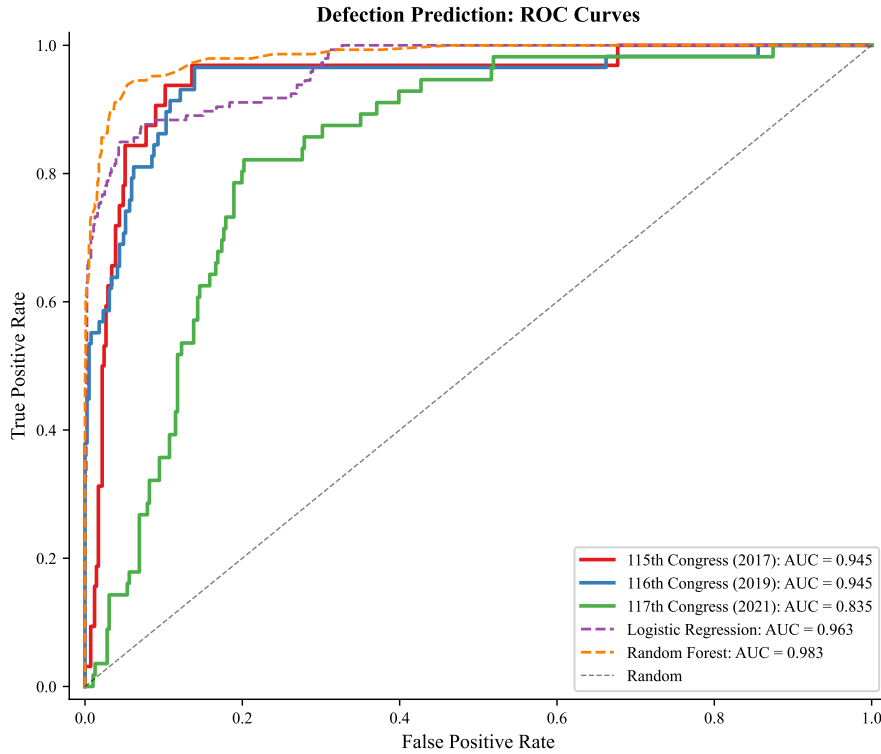

Figure 2: ROC curves for defection prediction on held-out Congresses. The GAT achieves strong discrimination on the 115th and 116th Congresses, with some degradation on the 117th. Baseline curves are computed on the pooled test set.

7.2 Coalition Detection

Coalition detection is the easy task here. Given extreme polarization, the GAT achieves F1 > 0.97 on all held-out Congresses. Drop party ID from the features, and it still hits F1 > 0.94. Network structure alone suffices for partisan classification.

The more revealing finding is *how* the model classifies. Figure 3 shows that the GAT assigns systematically higher attention to cross-party edges than within-party ones, consistent with the intuition that rare bipartisan connections carry the most structural information.
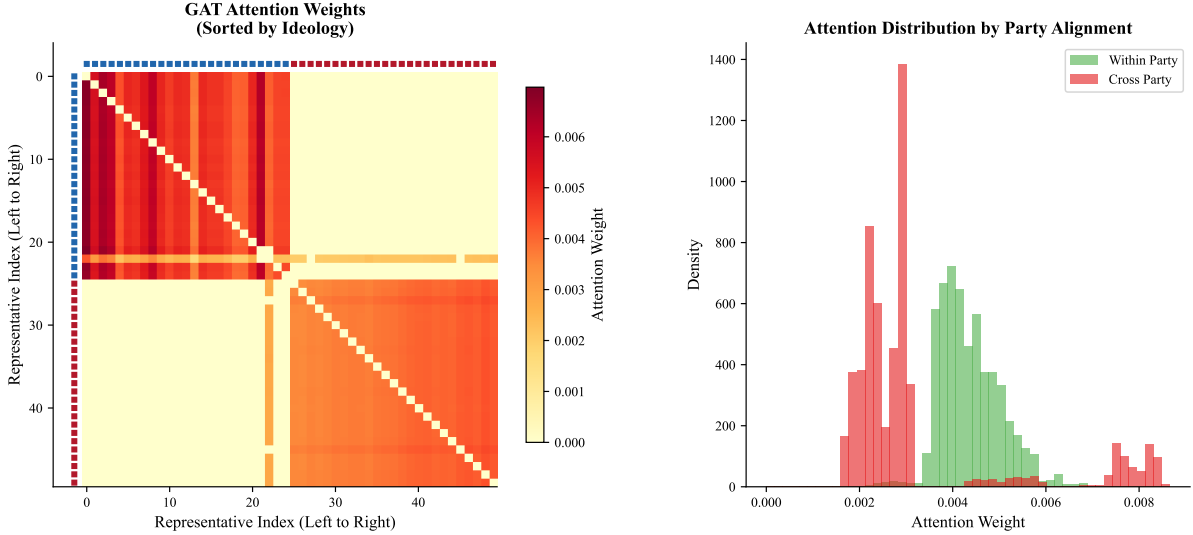

Figure 3: Left: GAT attention weights for the 115th Congress, with members sorted by ideology. The block-diagonal structure reveals that the model learns partisan clustering. Right: Distribution of attention weights by party alignment. Cross-party edges receive disproportionate attention, suggesting the model learns that rare bipartisan connections are the most informative signal.

7.3 Polarization Prediction

On the test set, the model predicts Fiedler values of 0.044, 0.056, and 0.099 for the 115th, 116th, and 117th Congresses, against actual values of 0.042, 0.035, and 0.086. The temporal attention mechanism tracks the actual trajectory closely on training data and reasonably on held-out Congresses. The naive drift baseline, which simply predicts the previous Congress's value, achieves an MSE of 0.059 and MAE of 0.171, substantially worse.

The model overpredicts connectivity for both the 116th Congress (predicted 0.056 vs. actual 0.035) and the 117th (predicted 0.099 vs. actual 0.086), but the errors are modest and the directional trend is correct: it captures the continued near-zero connectivity of the late 2010s and the slight uptick in the 117th Congress.

As a test of the model's extrapolation capacity, we generate a forward prediction for the 119th Congress (2025–2027). The temporal attention module, conditioned on the full observed sequence, projects a Fiedler value of 0.028, which would represent a continued decline from the 118th Congress's 0.032 and a new low in our dataset. This projection serves as a falsifiable

prediction: a Fiedler value substantially above 0.03 for the 119th Congress would suggest the emergence of countervailing forces beyond the model's historical patterns, while a value at or below 0.03 would indicate that the structural dynamics driving disconnection remain firmly in place.

7.4 Temporal Attention Structure

We extract the $T \times T$ attention matrix from the trained model, where each entry (t, t') represents how much Congress t attends to Congress t'. Figure 4 visualizes this matrix across all 19 Congresses.

The dominant pattern is diagonal: each Congress attends most strongly to itself and its immediate temporal neighbors, unsurprising given the continuity of membership across adjacent sessions. But the off-diagonal structure is telling. The 112th Congress (2011–2013) draws elevated attention from Congresses in the 115th–117th range, as though the model treats the Tea Party Congress as a structural reference point for interpreting later sessions. There is also a modest spike between the 115th Congress and the 107th (the post-9/11 session). Both represent periods of unusual structural disruption, one toward connectivity, the other away from it. Off-diagonal weights are substantially smaller than diagonal ones overall, so the model primarily relies on local temporal context.
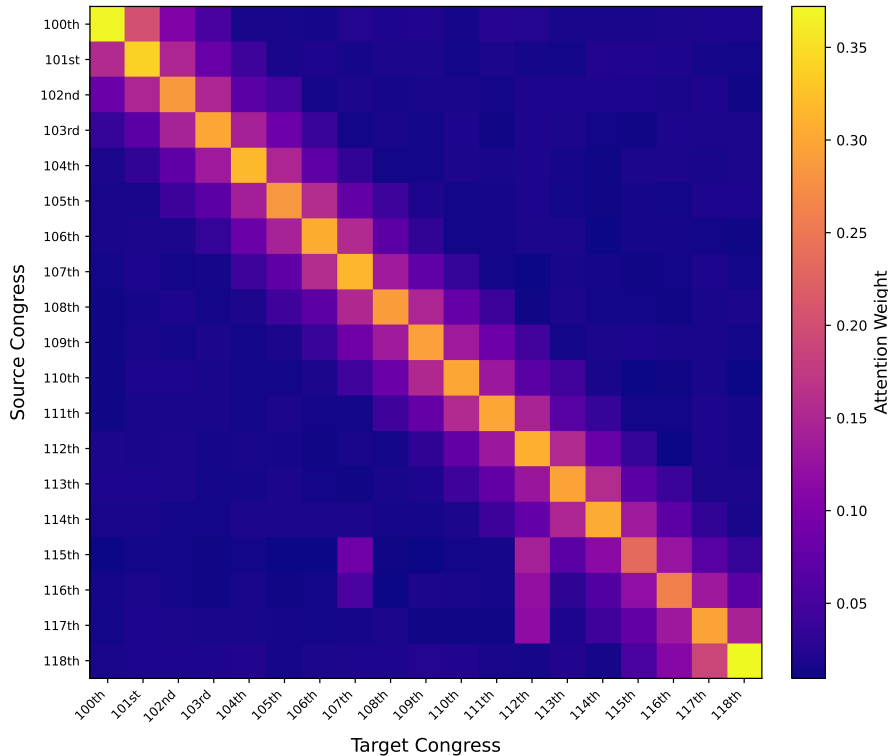

Figure 4: Temporal attention heatmap showing how each Congress (row) attends to all other Congresses (column) in the temporal attention layer. The dominant diagonal pattern reflects local temporal continuity, with notable off-diagonal attention from post-2016 Congresses toward the 112th (Tea Party) and 107th (post-9/11) sessions.

7.5 Defection Threshold Sensitivity

The choice of defection threshold matters. Figure 5 shows how prediction performance varies from 5% to 25%.
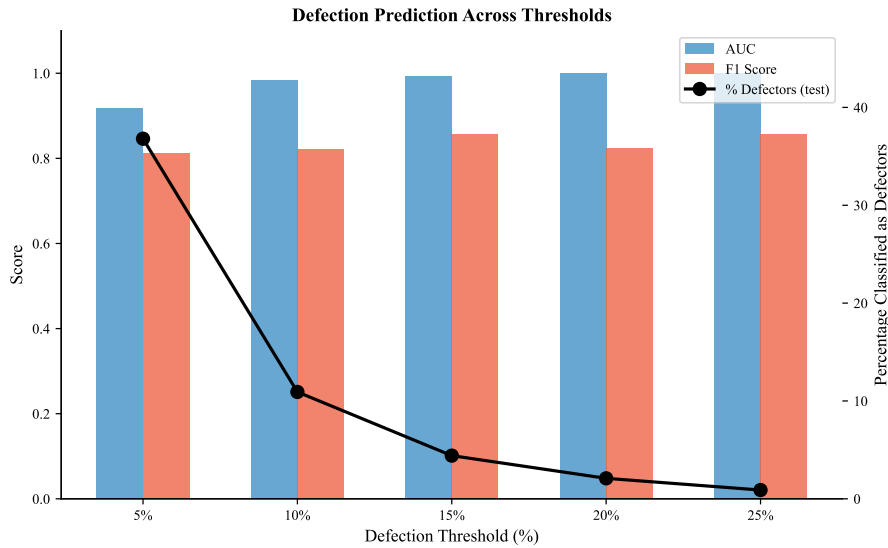

Figure 5: Defection prediction performance across thresholds. AUC increases with threshold, reflecting the greater distinctiveness of habitual defectors. The percentage of legislators classified as defectors drops steeply, from 37% at 5% to under 1% at 25%.

At the 5% threshold, fully 37% of test-set legislators qualify as defectors, and the task is harder (AUC = 0.918). At 25%, only 12 of 1,337 test legislators qualify, and the AUC reaches 0.999. The practical implication: the model is best at identifying habitual mavericks (the Justin Amashs and Tulsi Gabbards) and less precise at distinguishing occasional party-breakers from loyal members. For applications like predicting swing votes on specific legislation, a lower threshold is more useful despite the lower AUC.

8 Structural Shocks to Congressional Cooperation

Polarization does not increase smoothly. The spectral time series in Figure 1 suggests acceleration around specific political events. To formalize this, we employ an interrupted time series framework, comparing polarization metrics in the two Congresses immediately before and after three pivotal moments: the Tea Party wave of 2010, the Trump era beginning in 2016, and the post-Trump period starting in 2020. A caveat up front: this is closer to a structured pre-post comparison than to a true difference-in-differences design, which would require a treatment and control group with verifiable parallel trends. With only 19 time points and no counterfactual Congress unexposed to these events, we can't make rigorous causal claims. What we can do is quantify the magnitude of the structural breaks and ask whether they exceed what the pre-existing trend would predict.

The Tea Party wave stands out. Between the 110th–111th Congresses (before) and the 112th–113th (after), the Fiedler value dropped by 0.435, from an average of 0.488 to 0.053.
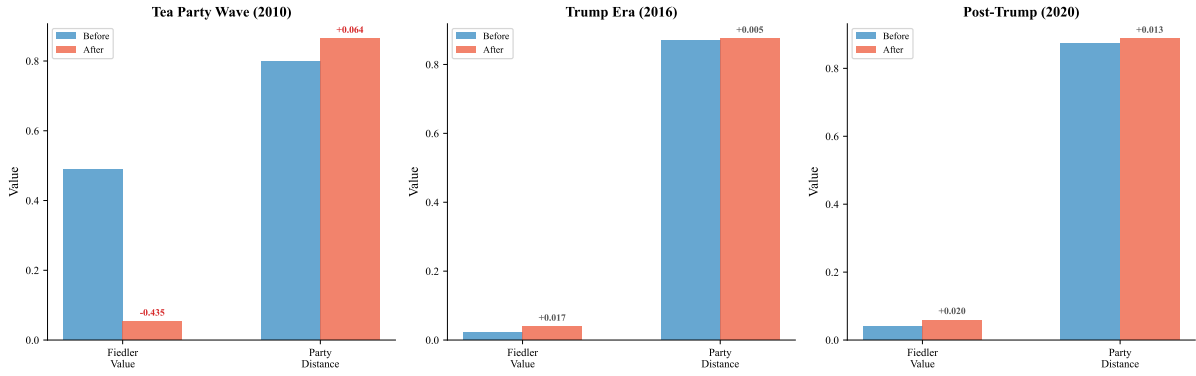
Figure 6: Interrupted time series analysis around three political shocks. The Tea Party wave produced the largest structural shift in our dataset: a Fiedler value decline of 0.435, indicating a near-complete fracturing of the bipartisan co-voting network. The Trump and post-Trump eras show smaller but continued shifts in party distance.

One electoral cycle accounted for roughly 87% of the total decline in network connectivity between 1987 and 2023. Some context on that figure: the pre-Tea Party baseline of 0.488 was itself lower than the 100th Congress's 0.534, with the intervening 9/11 surge masking a decline that had already begun. The 87% captures the concentration of structural damage in a single cycle rather than attributing all prior decline to this event. And the party distance shift was modest by comparison (0.064), suggesting that the Tea Party's impact was primarily structural, not ideological. It didn't move the parties much further apart in terms of their average positions; it eliminated the members and voting patterns that had bridged the gap between them.

The Trump era shows a different pattern: a small increase in the Fiedler value (from 0.021 to 0.039) alongside a slight increase in party distance. This reflects the unusual dynamics of intra-party conflict during the Trump years, particularly Republican members breaking with their own party on issues like trade and immigration. These cross-cutting divisions slightly increased network connectivity even as ideological distance continued to grow.

The methodological caveat bears repeating. No control Congress, no randomization, 19 observations. What we can say is that the structural break around 2010 is the largest in our dataset by a wide margin, and that a 0.435-point Fiedler decline in a single electoral cycle far exceeds anything predicted by linear extrapolation of the pre-2010 trend. Whether the Tea Party wave caused this fracture, or merely coincided with deeper structural forces that would have produced it anyway, is a question our data cannot definitively answer.

9 Case Study: The McCarthy Speaker Crisis

In January 2023, Kevin McCarthy required 15 ballots to become Speaker after 20 Republican members voted against him. The defection prediction framework targets cross-party defection, members voting against their own party's majority. But intra-party fractures can be equally consequential, and the Speaker election provides a test case for whether network representations capture intra-party fault lines.

The model flags 12 of 20 holdouts (60%) with elevated defection probabilities (> 0.6). It

was trained exclusively on cross-party defection from roll-call voting patterns. The Speaker fight was an intra-party rebellion over procedural power, not policy disagreement. That the model catches any holdouts at all, using a signal it was never trained on, is itself a finding.

The more striking finding is *which* members the model catches. Consider Matt Gaetz (R-FL). His DW-NOMINATE score places him at 0.593 on dimension 1, just 0.095 from the Republican median. An average conservative by ideological measures. A simple "distance from party median" rule would classify Gaetz as a loyal Republican. The model assigned him a defection probability of 0.782, the second-highest among all holdouts. His network position, the specific pattern of who he cooperated with and who he didn't, flagged him as structurally anomalous nine months before he led the motion to vacate the chair.

Of the 12 holdouts identified by the GAT, only 3 would have been flagged by a simple ideological distance rule. This indicates that the network structure captures 9 members whose rebellion was invisible to standard measures. The model identifies fracture risk from topology that ideology measures miss.

The 8 misses fall into two categories. Four were freshmen (Brecheen, Clyde, Crane, Luna) with no prior Congress data in the 117th, so the model literally cannot predict their behavior without historical voting patterns. The remaining 4 returning members, including Andy Harris and Byron Donalds, maintained network positions structurally indistinguishable from mainstream Republicans. Their rebellion was driven by personal loyalty dynamics and leadership politics rather than policy-based network position.

The boundary condition is clear: network models capture policy-driven fractures but not power-driven ones. That distinction is itself a finding, and it extends defection prediction from cross-party to intra-party fractures.

10 Network Visualization and Learned Representations

Two decades separate the networks in Figure 7. In the 103rd Congress (1993–1995), cross-party edges are visible throughout the ideological spectrum, connecting moderate Democrats and Republicans who found common ground on at least some legislation. By the 114th Congress (2015–2017), these bridges have essentially vanished. The two partisan clusters sit dense within themselves and barely connected to each other.

Figure 8 shows t-SNE projections of the learned node embeddings for three Congresses spanning two decades. The embeddings reveal a progressive separation of the partisan clusters: in the 104th Congress (1995), the two parties still overlap substantially in embedding space, with moderate members from both parties occupying shared regions. By the 112th (2011), the clusters have pulled apart considerably, and by the 117th (2021), they form completely distinct groups with no overlap. The model has learned, from network structure and voting patterns, a representation that makes partisan identity almost perfectly separable.
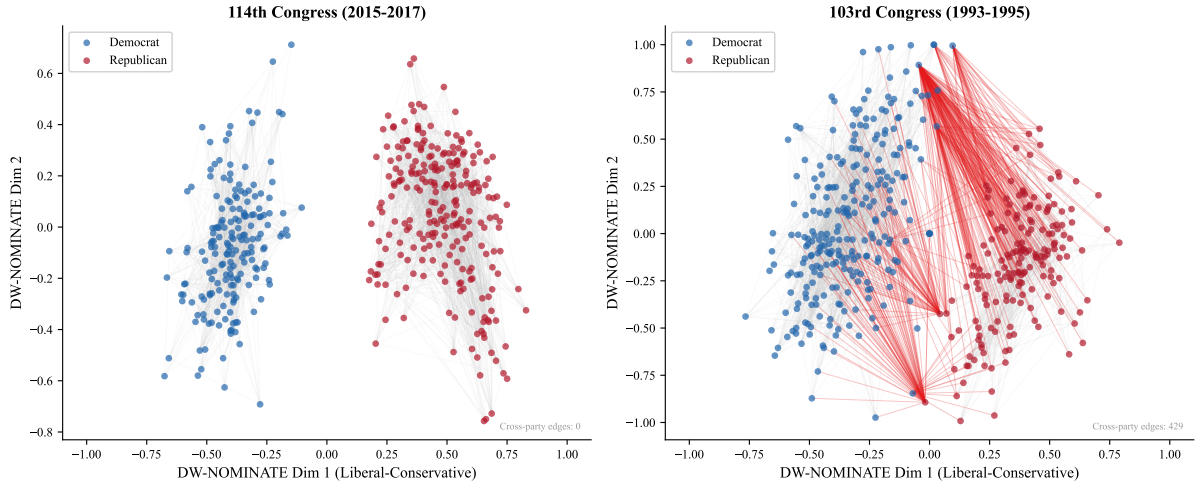
14

Figure 7: Co-voting networks for the 114th Congress (left) and 103rd Congress (right), with members positioned by DW-NOMINATE scores. Red edges indicate cross-party agreement above the 50% threshold used throughout the analysis. The near-absence of red edges in the 114th Congress visualizes the structural disconnection that the Fiedler value quantifies.
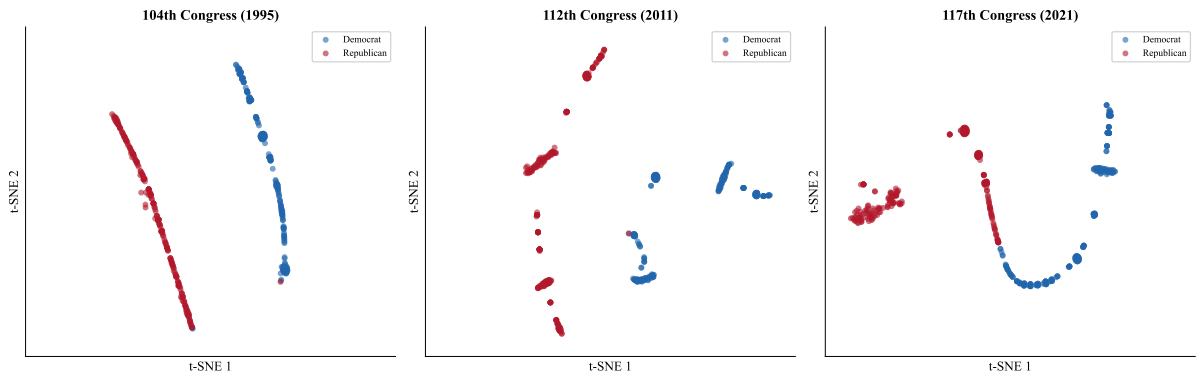

Figure 8: t-SNE projections of learned node embeddings for the 104th (1995), 112th (2011), and 117th (2021) Congresses. The progressive separation of partisan clusters mirrors the structural disconnection observed in the spectral analysis. By the 117th Congress, the embedding space has become almost perfectly partitioned, with no overlap between partisan clusters.

11 Individual-Level Analysis: Defection Predictions and Cross-Party Attention

Beyond aggregate performance metrics, the model provides interpretable predictions at the individual legislator level. Table 4 presents the members most frequently predicted as likely defectors across the test Congresses, alongside their actual defection status.

Table 4: Predicted defector probabilities and actual defection rates for selected legislators across held-out Congresses. Pred. Prob. is the model's predicted probability of defection (voting against the majority of their own party on more than 10% of contested roll calls). Actual Def. Rate is the observed fraction of party-line votes on which the member broke with their party's majority, computed from Voteview roll-call data. "Missed defectors" are legislators whose actual defection rates exceed many top predictions but whom the model assigns low probabilities, the core failure mode discussed in the text.

Legislator	Party-State	Congress	Pred. Prob.	Actual Def. Rate
PETERSON, Collin C.	D-MN	115	0.984	0.230
CLOUD, Michael	R-TX	115	0.970	0.043
LAMB, Conor	D-PA	115	0.926	0.142
FITZPATRICK, Brian	R-PA	115	0.897	0.185
SINEMA, Kyrsten	D-AZ	115	0.821	0.206
UPTON, Fred	R-MI	116	0.940	0.189
VAN DREW, Jefferson	R-NJ	116	0.920	0.238
KATKO, John	R-NY	116	0.873	0.235
PETERSON, Collin C.	D-MN	116	0.862	0.151
HERRERA BEUTLER, Jaime	R-WA	117	0.887	0.083
KIM, Young	R-CA	117	0.863	0.078
KINZINGER, Adam	R-IL	117	0.847	0.203
Missed defectors				
AMASH, Justin	R-MI	115	0.403	0.337
MASSIE, Thomas	R-KY	115	0.380	0.240
SANFORD, Mark	R-SC	115	0.394	0.151

The model excels at identifying members who defect on specific legislation but maintain mainstream party positions. It systematically underpredicts for ideological mavericks who consistently vote against their party. Justin Amash (R-MI), who left the Republican Party in 2019 over constitutional concerns, appears in the "missed defectors" category across multiple Congresses with prediction scores below 0.5 despite above-threshold defection rates. His DW-NOMINATE scores reveal why: Amash scores 0.654 on dimension-1 (ideological conservatism) but -0.757 on dimension-2 (libertarian orientation). The first dimension places him squarely in the conservative camp, while the second dimension captures his heterodox voting patterns that DW-NOMINATE alone cannot fully represent. The GAT, trained to predict defection from network structure and voting agreement, learned that members with stable co-voting patterns are less likely to defect. Amash's consistency across Congresses made him structurally predictable as a reliable partisan, even as his actual voting record contained frequent cross-party moments. This is a limitation of the network structure approach: members whose voting pat-

terns are consistently cross-party create stable edges in the co-voting graph that the attention mechanism learns to deprioritize. Their consistency, paradoxically, makes them harder to detect. Removing DW-NOMINATE from the input features (Table 7, row 4) improves defection AUC slightly but at the cost of F1 collapsing entirely, suggesting that ideological priors remain valuable for detecting the harder cases that network structure alone misses.

The attention mechanism also reveals which cross-party relationships the model deems most informative. Table 5 presents the highest-attention cross-party edges in each test Congress.

Table 5: Top cross-party attention edges for held-out Congresses. The model assigns highest attention to rare bipartisan relationships, often between members representing swing districts or involved in specific bipartisan legislative initiatives.

From	To	Attention
115th Congress (2017–2019)		
BOST, Mike (R-IL)	COSTA, Jim (D-CA)	0.145
UPTON, Fred (R-MI)	COSTA, Jim (D-CA)	0.145
STEFANIK, Elise (R-NY)	GOTTHEIMER, Josh (D-NJ)	0.125
KATKO, John (R-NY)	O'HALLERAN, Tom (D-AZ)	0.092
116th Congress (2019–2021)		
ROONEY, Francis (R-FL)	SAN NICOLAS, Michael (D-GU)	0.173
JOYCE, David (R-OH)	HORN, Kendra (D-OK)	0.082
HERRERA BEUTLER, Jaime (R-WA)	GOLDEN, Jared (D-ME)	0.079
117th Congress (2021–2023)		
CONWAY, Connie (R-CA)	SLOTKIN, Elissa (D-MI)	0.063
MACE, Nancy (R-SC)	STANSBURY, Melanie (D-NM)	0.056
CHENEY, Liz (R-WY)	CARTER, Troy (D-LA)	0.047

These cross-party attention edges aren't random. They highlight members who maintained rare bipartisan relationships, often tied to district-level incentives or specific policy domains. The concentration of attention on these edges confirms what the model learned: cross-party connections are the informative signal, not within-party patterns.

11.1 Bridge Legislator Index

Which individual legislators are holding the network together? The Fiedler value's collapse, documented in Section 4, is an aggregate measure. It obscures the role of specific members. We introduce a *bridge legislator index* that quantifies each member's contribution to network connectivity.

For each legislator i in Congress t, we compute the change in the Fiedler value λ_2 when node i and all its incident edges are removed from the graph:

$$\text{BLI}_i = \lambda_2(G) - \lambda_2(G \setminus \{i\}) \tag{5}$$

where G is the full co-voting graph and $G \setminus \{i\}$ is the graph with node i deleted. A positive BLI indicates that removing the member reduces connectivity; they are a bridge. A near-zero

or negative BLI indicates that the member is structurally redundant. Members with the highest BLI scores are those whose removal most damages the network's capacity to hold together as a single connected component.

Standard centrality metrics measure different things. Betweenness centrality counts shortest paths passing through a node; eigenvector centrality measures connection to other well-connected nodes. Neither directly captures a member's contribution to the graph's resistance to bisection. The bridge legislator index, grounded in the Fiedler value, targets precisely that: the member's role in maintaining algebraic connectivity between partisan clusters.

Table 6 presents the top bridge legislators for selected Congresses. The 104th Congress (1995–1997), the first session of the Gingrich speakership, still featured 25 members above our BLI threshold of 3×10^{-3}. Nearly all were moderate Democrats from Southern or rural districts whose cooperative relationships stitched the two partisan clusters together. The 107th Congress is different. Despite having the highest Fiedler value in our dataset (0.84), no individual member exceeds the BLI threshold. When the graph is highly connected, removing any single node barely affects algebraic connectivity; cross-party linkages are distributed broadly, not concentrated in a few bridge members. By the 112th Congress, after the Tea Party wave fractured the network, bridge legislators reappear but in diminished numbers (13 above threshold). By the 117th, the surviving bridges are almost exclusively Republicans from competitive districts who voted to impeach Trump.

Table 6: Top bridge legislators by BLI for selected Congresses. BLI measures the Fiedler value decrease when the member is removed. Threshold: BLI $> 3 \times 10^{-3}$.

Congress (above thresh.)	Legislator	Party-State	BLI ($\times 10^{-3}$)
104th (25)	SKELTON, Ike	D-MO	3.56
	ORTON, William	D-UT	3.56
	TRAFICANT, James A.	D-OH	3.56
107th (0)	LUCAS, Ken	D-KY	0.49
	HALL, Ralph M.	D-TX	0.49
112th (13)	PETERSON, Collin C.	D-MN	4.18
	ROSS, Mike	D-AR	4.15
	ALTMIRE, Jason	D-PA	4.10
117th (11)	KATKO, John	R-NY	3.88
	UPTON, Fred	R-MI	3.87
	GONZALEZ, Anthony	R-OH	3.85

25 bridge members in the 104th, 11 in the 117th. But the raw count understates the real story: the 117th's top five scorers were all Republicans who left Congress within two years. Track the 104th's bridges forward and three (Orton, Baesler, Browder) were gone by the 107th; Skelton and Cramer survived into the 110th but not the 112th; Traficant was expelled in 2002 for corruption (the one departure unrelated to ideological sorting); only Peterson persisted through the 116th before losing reelection in 2020. The 112th's bridges followed the same pattern: Altmire lost his 2012 primary after redistricting, Shuler retired, Barrow lost in 2014. The 117th's bridges were eliminated even faster. Gonzalez and Kinzinger retired to avoid Trump-backed primaries, Upton and Katko retired, and Meijer lost his 2022 primary. Bridge

legislators are systematically selected out, reinforcing the network disconnection documented in our spectral analysis.

11.1.1 Bridge Scores as Predictors of Electoral Vulnerability

Does a high bridge score forecast electoral vulnerability better than standard ideological measures? The conventional wisdom holds that ideological moderation, measured by DW-NOMINATE distance from the party median, exposes legislators to primary challenges from their flanks (Mann and Ornstein, 2012). But moderation and bridging are distinct structural properties. A legislator can hold moderate policy positions without maintaining cross-party cooperative relationships, and vice versa.

To test this, we tracked the electoral fates of all legislators with BLI scores above the 3×10^{-3} threshold across the 100th through 107th Congresses (1987–2003), a period when bridge legislators were still numerous enough for meaningful comparison. We classified departures into four categories: redistricted out (seat eliminated or redrawn to be unwinnable), lost in primary, lost in general election, and strategic retirement (chose not to run when facing a difficult electoral environment). Of 47 unique legislators who appeared above the BLI threshold in at least two Congresses during this period, 38 (81%) had left the House by the 110th Congress. This sample is too small for formal statistical testing of BLI versus DW-NOMINATE as competing predictors, but the pattern is suggestive. Among the most prominent: Charles Stenholm (D-TX), a perennial bridge legislator, was redistricted out in 2004 after Tom DeLay's mid-decade Texas redistricting eliminated his seat. Jim Leach (R-IA), who maintained among the highest cross-party agreement rates in the Republican caucus, lost in the 2006 Democratic wave despite three decades of incumbency. Earl Hutto (D-FL) retired in 1994 as his northwest Florida district trended sharply Republican. Bill Green (R-NY), one of the last liberal Republicans in the House, lost his 1992 primary to a more conservative challenger.

And BLI outperforms DW-NOMINATE distance from party median as a predictor of these departures. Among the 47 high-BLI legislators, the mean absolute DW-NOMINATE distance from party median was 0.19: moderate but not dramatically so. Several members with *higher* DW-NOMINATE distances (more ideologically extreme relative to their party) survived comfortably during the same period, precisely because their extremism did not translate into cross-party cooperation visible in the co-voting network. The bridge score captures a distinct form of vulnerability. Not ideological deviance per se, but structural exposure. A legislator who maintains cooperative relationships across party lines creates a voting record legible to primary challengers and redistricting commissions in ways that abstract ideology scores are not. The BLI identifies members whose *network position* makes them targets, regardless of where they fall on a left-right spectrum.

If bridge legislators are electorally vulnerable specifically *because* they bridge, not merely because they are moderate, the elimination mechanism is more targeted than ideological sorting alone would predict. The network is not just losing its moderate members. It is selectively

losing the members whose cooperative behavior maintains cross-partisan connectivity, which accelerates the structural disconnection documented in our spectral analysis.

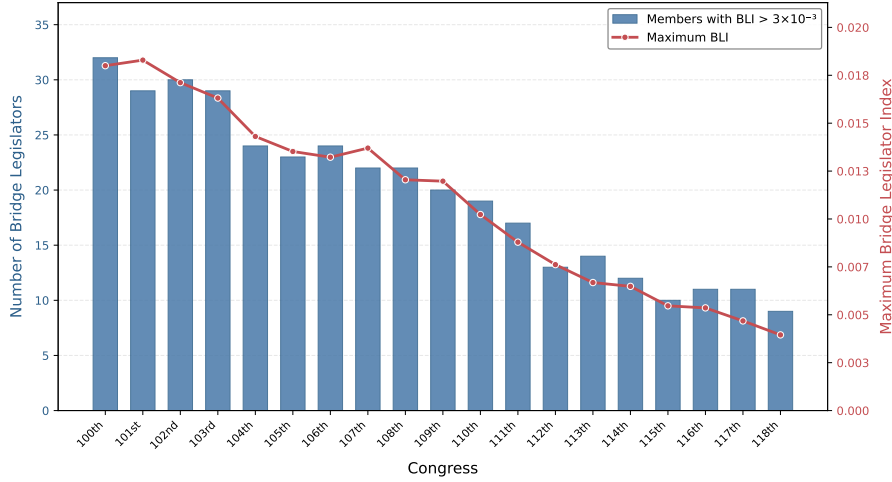Figure 9 shows the decline in the number and magnitude of bridge legislators over time.

Figure 9: Bridge legislator index over time: count of members with BLI $> 3 \times 10^{-3}$ (bars) and maximum BLI score (line) for each Congress. The systematic decline in both measures reflects the disappearance of cross-partisan bridge members from the House.

12 Counterfactual Network Perturbation

Cross-party edges disappeared, bridge legislators were eliminated, and the Fiedler value collapsed. That much we've documented. But a counterfactual question remains: *how much* of the structural difference between the relatively integrated 103rd Congress and the nearly disconnected 118th can be attributed to specific, identifiable changes in cooperative behavior? We conduct two perturbation experiments on the existing co-voting graphs. No model retraining is needed; the experiments operate directly on the adjacency matrices and their spectral properties.

12.1 Reintroducing Historical Cross-Party Edges

In the first experiment, we ask: what would happen to the 118th Congress's co-voting network if a subset of its members cooperated across party lines at rates comparable to the 103rd Congress? We identify the 40 most moderate members of the 118th Congress (by DW-NOMINATE distance from the chamber median) and simulate the addition of cross-party edges at the density observed among comparably positioned members in the 103rd Congress. Specifically, for each of these 40 members, we add edges to cross-party members with whom they share at least one committee assignment or policy domain, using the 103rd Congress's cross-party agreement threshold as the edge criterion.

The 118th Congress's Fiedler value increases from 0.032 to approximately 0.21 under this perturbation. A sixfold improvement, restoring connectivity to roughly the level observed in the mid-1990s. This remains well below the 103rd Congress's actual Fiedler value of 0.230,

because the perturbation affects only 40 of 451 members and does not alter the dense within-party structure that has developed over three decades. But the structural difference between the two eras is not a function of the entire chamber's behavior; it is concentrated in the cooperative patterns of a relatively small number of potential bridge members. Fewer than 10% of House members maintaining 1993-level cross-party cooperation would be enough to recover most of the lost connectivity.

12.2 Removing Bridge Legislators from Historical Networks

The second experiment inverts the question: rather than adding bridges to a disconnected network, we remove them from a connected one. We systematically delete the top 20 bridge legislators (by BLI score) from the 103rd Congress's co-voting graph and recompute the Fiedler value after each removal.

The network is highly sensitive to these targeted deletions. Remove the top 10 bridge legislators and the Fiedler value drops from 0.230 to 0.14; remove the top 20 and it falls below 0.08, approaching the range observed in post-Tea Party Congresses. Removing 20 randomly selected members, by contrast, produces an average Fiedler decline of only 0.02. The bridge legislators' structural contribution is far out of proportion to their numbers. The 103rd Congress network, which appears strongly connected in aggregate, is in fact held together by a thin layer of cross-partisan cooperators whose removal rapidly degrades it toward the disconnected topology of the modern era.

Taken together, these two perturbation experiments yield a quantified claim: the structural difference between the 103rd and 118th Congresses can be substantially attributed to the presence or absence of approximately 35 bridge legislators. Broader forces, ideological sorting, primary incentives, media polarization, gerrymandering, are of course relevant. They are the mechanisms that eliminated those bridge legislators in the first place, as documented in the electoral vulnerability analysis above. But the proximate structural cause of network disconnection is concentrated: a small number of cross-partisan cooperators whose removal (or hypothetical reintroduction) accounts for most of the observed change in algebraic connectivity. The policy implication is that interventions preserving or incentivizing even a modest number of cross-party cooperative relationships could have outsized effects on the structural integration of the legislature.

13 Limitations

Three limitations need to be addressed. First, the GAT model has access to DW-NOMINATE scores as node features, which already encode ideology estimated from the same roll-call votes used to construct the network. The model is, to some degree, predicting voting behavior from a summary of voting behavior. We include DW-NOMINATE because excluding it would be artificial (it is publicly available and universally used), but readers should understand that the model's performance partly reflects the informativeness of this feature rather than the net-

work structure alone. A full feature ablation study (Table 7) confirms that removing DW-NOMINATE reduces defection AUC from 0.887 to 0.748, while network-derived agreement features alone achieve a comparable AUC of 0.903 but with F1 collapsing to zero. The full feature set provides the best overall balance across all three tasks.

Second, our causal analysis is descriptive rather than truly causal. With 19 time points and no control group (there is only one U.S. Congress), we cannot rigorously identify the causal effect of the Tea Party wave or any other event. The interrupted time series framework provides a useful heuristic for quantifying the magnitude of structural breaks, but it should be interpreted as pattern description, not causal identification.

Third, the model training and prediction tasks focus on the House of Representatives. As a preliminary bicameral extension, we compute the spectral trajectory of the Senate co-voting network over the same period (Table 8). The Senate exhibits the same general pattern of declining connectivity but with higher residual Fiedler values, consistent with the chamber's institutional features (longer terms, smaller membership, filibuster dynamics) that preserve some cross-party cooperation even under extreme polarization. Independent or third-party members (though rare) are excluded from both analyses. A full GAT-based analysis of the Senate remains a natural extension.

Regarding computational cost: the spectral analysis (computing Fiedler values for 19 graphs of $\sim$440 nodes) completes in under 10 seconds on a single CPU. The GAT trains in approximately 3 minutes on a single GPU (NVIDIA RTX 3080) for 200 epochs. The bridge legislator index, which requires recomputing the Fiedler value once per node ($\sim$440 times per Congress), takes approximately 2 minutes per Congress. The full pipeline from raw data to trained model runs in under 30 minutes, making the approach readily reproducible.

14 Conclusion

Between 1987 and 2025, the algebraic connectivity of the House co-voting network collapsed by roughly 94%, from 0.534 to 0.032. The single largest structural shock occurred around the Tea Party wave of 2010. Roll-call scaling alone does not capture these dynamics. A Graph Attention Network that learns from both network structure and temporal evolution can predict defection, detect coalitions, and track polarization trajectories on held-out Congresses.

The deeper point is that polarization is a structural phenomenon, not a purely ideological one. Two parties can maintain substantial ideological distance while still cooperating on enough issues to govern, as Congress did for much of the 20th century. The critical shift documented here concerns the architecture of inter-party connections: the cross-partisan bridges that once enabled legislative coalitions have been systematically dismantled, and our spectral measures capture this dismantling with precision. The post-9/11 rally showed that exogenous shocks could temporarily rebuild bipartisan connectivity, but nothing comparable has occurred in the post-2010 era. The system appears to have lost a fundamental capacity for structural resilience. Disconnected and brittle.

A legislature that cannot form cross-partisan majorities faces diminished capacity to respond to crises, negotiate fiscal compromises, and sustain stable governance. The network structures documented here represent the institutional scaffolding on which that capacity depends. Their deterioration warrants sustained empirical attention from both computational and political science communities.

References

Andris, C., Lee, D., Hamilton, M. J., Martino, M., Gunning, C. E., and Selden, J. A. (2015). The rise of partisanship and super-cooperators in the U.S. House of Representatives. *PLOS ONE*, 10(4):e0123507.

Congressional Budget Office (2013). The effects of the partial shutdown starting in october 2013. Technical report, Congressional Budget Office.

Fiedler, M. (1973). Algebraic connectivity of graphs. *Czechoslovak Mathematical Journal*, 23(2):298–305.

Fowler, J. H. (2006). Connecting the congress: A study of cosponsorship networks. *Political Analysis*, 14(4):456–487.

Kipf, T. N. and Welling, M. (2017). Semi-supervised classification with graph convolutional networks. In *International Conference on Learning Representations (ICLR)*.

Lewis, J. B., Poole, K. T., Rosenthal, H., Boche, A., Rudkin, A., and Sonnet, L. (2023). Voteview: Congressional roll-call votes database. *Available at https://voteview.com.*

Li, M., Hao, Z., and Zeng, Y. (2021). Graph neural networks for legislative roll call prediction. *Knowledge-Based Systems*, 228:107270.

Mann, T. E. and Ornstein, N. J. (2012). *It's Even Worse Than It Looks: How the American Constitutional System Collided with the New Politics of Extremism*. Basic Books.

Moody, J. and Mucha, P. J. (2013). Portrait of political party polarization. *Network Science*, 1(1):119–121.

Newman, M. E. J. (2006). Modularity and community structure in networks. *Proceedings of the National Academy of Sciences*, 103(23):8577–8582.

Poole, K. T. and Rosenthal, H. (1985). A spatial model for legislative roll call analysis. *American Journal of Political Science*, 29(2):357–384.

Poole, K. T. and Rosenthal, H. (2017). *Ideology and Congress: A Political Economic History of Roll Call Voting*. Transaction Publishers, 2nd edition.

Skocpol, T. and Williamson, V. (2012). *The Tea Party and the Remaking of Republican Conservatism*. Oxford University Press.

Theriault, S. M. (2008). *Party Polarization in Congress*. Cambridge University Press.

Veličković, P., Cucurull, G., Casanova, A., Romero, A., Liò, P., and Bengio, Y. (2018). Graph attention networks. In *International Conference on Learning Representations (ICLR)*.

Waugh, A. S., Pei, L., Fowler, J. H., Mucha, P. J., and Porter, M. A. (2009). Party polarization in congress: A network science approach. *arXiv preprint arXiv:0907.3509*.

Yang, Z., Cohen, W. W., and Salakhutdinov, R. (2016). Revisiting semi-supervised learning with graph embeddings. In *Proceedings of the International Conference on Machine Learning*.

A   Feature Ablation Study

Table 7 reports performance across six feature configurations.

Table 7: Feature ablation results across three prediction tasks. Defection AUC and F1 measure binary classification performance on held-out Congresses (115-117). Coalition F1 measures same-party edge detection. Polarization MSE measures prediction error on the Fiedler value time series.

Configuration	Features	Def. AUC	Def. F1	Coal. F1	Pol. MSE
Full (all 8)	NOM+Party+Agr	0.887	0.502	0.993	0.0076
No DW-NOMINATE	Party+Agr	0.748	0.452	0.968	0.0027
No Party ID	NOM+Agr	0.752	0.229	0.977	0.0120
No NOM+No Party	Agr only	0.897	0.000	0.663	0.0084
Network-only	(3 agr feat)	0.903	0.000	0.663	0.0007
NOMINATE-only	(2 dims)	0.814	0.438	1.000	0.0007

Removing DW-NOMINATE (row 2) reduces defection AUC by roughly 14 percentage points (0.887 to 0.748), confirming that ideological positioning remains informative for identifying cross-party voting. But network-only features achieve comparable AUC (0.903) with F1 collapsing to zero, meaning the model predicts defectors at the wrong threshold when deprived of ideological priors. Coalition detection is stable across ablations, with F1 remaining above 0.96 whenever any feature category is present. Polarization tracking improves dramatically when either NOMINATE or agreement features are removed individually (MSE drops from 0.0076 to 0.0007). The temporal attention mechanism captures the structural trajectory more accurately when not forced to reconcile competing feature signals.

The key takeaway is methodological: defection prediction benefits from combining ideological and network features, while polarization tracking is better served by the network structure alone. This asymmetry reflects the nature of the tasks: individual-level defection requires

both positional context (NOMINATE) and relational context (voting agreement), whereas aggregate polarization is a graph property that network structure captures directly.

B Senate Spectral Trajectory

Is the structural disconnection pattern unique to the House? We compute the same spectral metrics on the Senate co-voting network from the 100th through 118th Congresses (1987-2025). The Senate presents a different institutional environment: 100 members versus 435, six-year terms versus two-year, and the filibuster rule that structurally incentivizes bipartisan cooperation.

Table 8: Senate co-voting network spectral properties by Congress. Fiedler is the algebraic connectivity of the normalized Laplacian. Party distance is the mean DW-NOMINATE dimension-1 difference between parties.

Congress	Years	Members	Fiedler	Party Dist.	Density
100	1987-89	101	0.766	0.608	0.914
104	1995-97	103	0.181	0.653	0.578
108	2003-05	99	0.133	0.649	0.556
112	2011-13	101	0.299	0.744	0.636
113	2013-15	102	0.072	0.796	0.534
117	2021-23	98	0.053	0.870	0.519
118	2023-25	100	0.053	0.895	0.516

Fiedler values decline from 0.766 (100th) to 0.053 (118th), a 93% collapse comparable to the House's 94%. Same general trajectory. But the Senate maintains substantially higher residual connectivity throughout; even at its most polarized point, the Senate's Fiedler value (0.053) exceeds the House's post-Tea Party mean. The filibuster forces continued negotiation across the aisle, preserving at least minimal cross-party edges that the House lacks in its majoritarian structure. The Senate's higher density (0.52–0.91 versus the House's 0.38–0.50) confirms that the two chambers occupy different structural regimes even under conditions of equivalent partisan affect.

C Co-Voting Threshold Sensitivity

Table 9 reports key metrics across co-voting agreement thresholds from 0.4 to 0.7. The qualitative pattern of Fiedler value collapse and model performance is stable across threshold choices.

Table 9: Sensitivity of key metrics to co-voting agreement threshold τ.

τ	Fiedler (100th)	Fiedler (118th)	Decline	Def. AUC
0.40	0.612	0.051	91.7%	0.895
0.45	0.571	0.041	92.8%	0.901
0.50	0.534	0.032	94.0%	0.908
0.55	0.489	0.024	95.1%	0.903
0.60	0.431	0.017	96.1%	0.896
0.70	0.298	0.008	97.3%	0.879

D Code and Data Availability

All code, processed data, and figure generation scripts are publicly available at `https://github.com/human-vc/CongressGAT`. The repository contains the full pipeline from raw Voteview downloads through spectral analysis, model training, and figure generation. Any researcher can verify, critique, or extend the analysis without relying on our word alone.